

Variational quantum Gibbs state preparation with a truncated Taylor series

Youle Wang^{1,2}, Guangxi Li^{1,2}, and Xin Wang^{1*}

¹*Institute for Quantum Computing, Baidu Research, Beijing 100193, China and*

²*Centre for Quantum Software and Information,
University of Technology Sydney, NSW 2007, Australia*

(Dated: May 19, 2020)

The preparation of quantum Gibbs state is an essential part of quantum computation and has wide-ranging applications in various areas, including quantum simulation, quantum optimization, and quantum machine learning. In this paper, we propose variational hybrid quantum-classical algorithms for quantum Gibbs state preparation. We first utilize a truncated Taylor series to evaluate the free energy and choose the truncated free energy as the loss function. Our protocol then trains the parameterized quantum circuits to learn the desired quantum Gibbs state. Notably, this algorithm can be implemented on near-term quantum computers equipped with parameterized quantum circuits. By performing numerical experiments, we show that shallow parameterized circuits with only one additional qubit can be trained to prepare the Ising chain and spin chain Gibbs states with a fidelity higher than 95%. In particular, for the Ising chain model, we find that a simplified circuit ansatz with only one parameter and one additional qubit can be trained to realize a 99% fidelity in Gibbs state preparation at inverse temperatures larger than 2.

I. INTRODUCTION

Quantum state preparation is an integral part of quantum computation. In the near future, quantum computers will become quantum state preparation factories for various tasks. One central task in quantum state preparation is to prepare the quantum Gibbs or thermal state of a given Hamiltonian. The reason is that quantum Gibbs states not only can be used to study many-body physics, but also can be applied to quantum simulation [1], quantum machine learning [2, 3], and quantum optimization [4]. In particular, sampling from well-prepared Gibbs states of Hamiltonians can be applied in solving combinatorial optimization problems [5], solving semi-definite programs [6], and training quantum Boltzmann machines [7].

The preparation of the desired initial state is a difficult problem in general. It is well-known that finding ground states of Hamiltonians is QMA-hard [8]. Gibbs state preparation at arbitrary low temperature could be as hard as finding the ground state [9]. Several methods have been proposed to sample from thermal states on quantum computers. These methods use quantum computing techniques, including quantum rejection sampling [10, 11], quantum walk [12], dynamics simulation [13–15], dimension reduction [16]. Although, in the worst case, the costs of these methods require could be exponential in expectation, they can be efficient when some conditions are satisfied. Such as the ratios between the partition functions of the infinite temperature states and the Gibbs state is at most polynomially large [17], and the gap of the Markov chain that describes the quantum walk is polynomially small [18, 19]. However, these methods require the use of complex quantum subroutines such as quantum phase estimation, which are costly and hard to implement on near term quantum computers.

One main goal of our research is to prepare quantum Gibbs states with near-term devices by reducing the required quantum resources including quantum circuit depth and width. One feasible scheme for this purpose is to employ variational quantum algorithms [20]. Several vari-

*wangxin73@baidu.com

ational quantum algorithms have been proposed for solving linear systems of equations [21–23], Hamiltonian ground and excited states preparation [24, 25], quantum state diagonalization [26], quantum state fidelity estimation [27] etc. These variational quantum algorithms involve evaluating and optimizing the loss function that depends on the parameters of a sequence of quantum gates. The loss function is evaluated on the quantum devices and then iteratively optimized on the classical devices. Variational quantum algorithms manage to reduce the required quantum resources at the expense of additional classical optimization, hence they could be implemented on near-term quantum computers [20, 22, 23].

In this paper, we propose variational algorithms for preparing the quantum Gibbs state. The quantum Gibbs state for a Hamiltonian H is defined as a density operator $\rho_G = e^{-\beta H} / \text{Tr}(e^{-\beta H})$, where β is the inverse temperature $\beta = 1/k_B T$. A key feature of the Gibbs state is that it minimizes the free energy [28]. Recall that free energy \mathcal{F} of a system is associated with the density ρ , further, and it is given by $\mathcal{F}(\rho) = \text{Tr}(H\rho) - \beta^{-1}S(\rho)$, where $S(\rho)$ is the von Neumann entropy. Hence, one could find the Gibbs state via minimizing the free energy \mathcal{F} and ρ_G can be approximately prepared by the following variational principle of Gibbs state:

$$\rho_G \approx \text{argmin}_{\theta} \mathcal{F}(\rho(\theta)), \quad (1)$$

where $\rho(\theta)$ is prepared with parameterized circuits. To develop a variational algorithm on near-term devices, one major obstacle for the above free energy evaluation is the von Neumann entropy estimation. Wu and Hsieh [29] proposed a variational approach by using Rényi entropy estimation [30] and thermofield double states, while Chowdhury et al. [31] proposed entropy estimation method using tools such as quantum amplitude estimation and linear combination of unitaries. In contrast, we take a truncated version of the free energy as loss function where the von Neumann entropy is truncated at order K , i.e., $S_K(\rho)$. We show that the truncated entropy can be represented as a linear combination of higher order state overlap, which can be estimated via certain subroutines. In particular, we focus on the 2-truncated free energy and regard it as the loss function. As a notable example, we show that the trained state via optimizing this loss function can be used to approximate the Gibbs state with fidelity at least 95% for the Ising chain and XY spin- $\frac{1}{2}$ chain models. Particularly, our algorithm can prepare Ising chain Gibbs states with fidelity at least 99% at low temperatures. To better guarantee the behaviour of our variational quantum algorithm, we prove the convexity of 2-truncated free energy and then apply the gradient-based method to optimize it.

Our paper is organized as follows. In Sec. II, we describe our main result of this paper. First, we present the variational algorithm for Gibbs state preparation; Next, we give an error analysis for our algorithm. Third, we elaborate in detail the computation of the analytical gradient of the loss function for optimization. In Sec. III, we numerically demonstrate the effectiveness of our algorithm, especially in lower temperature, via targeting the Gibbs state preparation of Ising model and XY spin-1/2 model. Additionally, we further explore a more sophisticated ansatz with only one parameter and show its powerful ability for Gibbs state preparation of Ising model. In Sec. IV, we complete the paper with discussions.

II. MAIN RESULTS

A. Hybrid quantum-classical algorithm for Gibbs state preparation

The Gibb state for a quantum Hamiltonian H is defined as the density operator

$$\rho = \frac{\exp(-\beta H)}{\text{Tr}(\exp(-\beta H))}. \quad (2)$$

We recall that the free energy of a system described by a density operator ω is given by

$$\mathcal{F}(\omega) = \text{Tr}(\omega H) - \beta^{-1} S(\omega), \quad (3)$$

where $\beta = (k_B T)^{-1}$ is the inverse temperature of the system, k_B is the Boltzmann's constant, and $S(\rho) := -\text{Tr} \rho \ln \rho$ is the von Neumann entropy of ρ .

As the Gibbs state minimizes the free energy of the Hamiltonian H , it holds that

$$\rho = \text{argmin}_{\omega} \mathcal{F}(\omega). \quad (4)$$

Therefore, if we could generate parametrized quantum states $\omega(\theta)$ and find a way to measure or estimate the loss function $\text{Tr}(\omega H) - k_B T \cdot S(\omega)$, then one could design variational algorithms via the optimization over θ [29, 31]. However, determining the von Neumann entropy of a quantum state on near-term quantum devices is quite challenging. Existing quantum algorithms for estimating certain entropic quantities [31–33] are not suitable for our purpose of using near-term quantum devices since they either have an explicit polynomial dependence on the Hilbert-space dimension of quantum system or require certain oracle assumption. Recently, the authors of [31] propose a procedure for estimating the von Neumann entropy and free energy that uses tools such as quantum amplitude estimation [34], density matrix exponentiation [35], and techniques for approximating operators by a linear combination of unitaries.

To design a suitable and efficient variational quantum algorithm for near-term quantum devices, we design a novel loss function in the similar spirit of the free energy. This new loss function utilizes the truncated Taylor series and in particular can be efficiently estimated on near-term quantum devices. After optimizing the parametrized circuits to minimize this loss function, the output state approximates the target Gibbs state with a high fidelity. The overlap, in terms of fidelity, between the output state and the Gibbs state increases as the truncation order K increases. Note that the subroutine of loss evaluation occurs on the quantum devices, and the procedure of optimization is entirely classical. Therefore, the classical optimization tools such as the gradient-based or gradient-free methods can be employed in the optimization loop.

The goal is to design and optimize the variational quantum circuits that minimize the loss function. In general, the variational quantum circuit contains alternately a series of parametrized single qubit Pauli rotation operators and CNOT/CZ gates [36]. Here we follow this circuit pattern and mainly use Pauli-Y rotation operators and CNOT gates. For the optimization part, a variety of approaches have been proposed to optimize such variational quantum circuits, including Nelder-Mead [37, 38], Monte-Carlo [39], quasi-Newton [37], gradient descent [40], and Bayesian methods. Here we choose ADAM [41] as our gradient-based optimizer. For the loss evaluation part, the core of our idea is to truncate the von Neumann entropy as a linear combination of higher order state overlaps, i.e., $\text{Tr}(\rho^k)$, and estimate each $\text{Tr}(\rho^k)$ respectively. After the hybrid quantum-classical optimization, the output state thus approximates the target Gibbs state.

The overall hybrid algorithm (see Algorithm 1) is as follows (see Fig. 1 for the general scheme). Variational quantum algorithm for general truncation order K is deferred to the Appendix I.

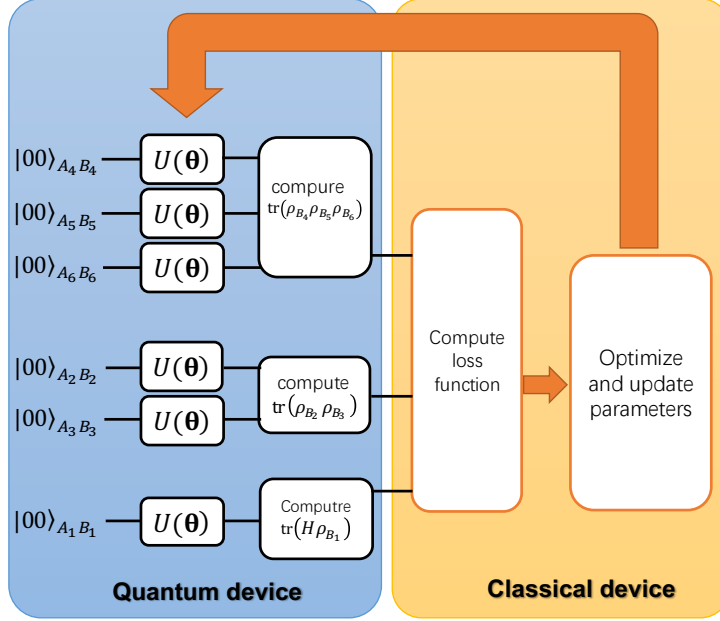


FIG. 1: Schematic representation of the variational quantum Gibbs state preparation with truncation order 2. Here in the quantum device, registers A_2, B_2, A_3, B_3 are used to evaluate $\text{Tr}(\rho_{B_2}\rho_{B_3})$ and registers $A_4, B_4, \dots, A_6, B_6$ are used to evaluate $\text{Tr}(\rho_{B_4}\rho_{B_5}\rho_{B_6})$. Specifically, if all $U(\theta)$'s are identical, we denote these partial trace as $\text{Tr}(\rho_B^2)$ and $\text{Tr}(\rho_B^3)$, respectively for abbreviation.

Algorithm 1 Variational quantum Gibbs state preparation with truncation order 2

- 1: Input: choose the ansatz of unitary $U(\theta)$, tolerance ε , truncation order 2, and initial parameters of θ ;
 - 2: Compute coefficients C_0, C_1, C_2 according to Eq. (6).
 - 3: Prepare the initial states $|00\rangle$ in registers AB and apply $U(\theta)$.
 - 4: Measure and compute $\text{Tr}(H\rho_{B_1})$ and compute the loss function $L_1 = \text{Tr}(H\rho_{B_1})$;
 - 5: Measure and compute $\text{Tr}(\rho_{B_2}\rho_{B_3})$ via Destructive Swap Test and compute the loss function $L_2 = -\beta^{-1}C_1 \text{Tr}(\rho_{B_2}\rho_{B_3})$;
 - 6: Measure and compute $\text{Tr}(\rho_{B_4}\dots\rho_{B_6})$ via higher order state overlap estimation and compute the loss function $L_3 = -\beta^{-1}C_2 \text{Tr}(\rho_{B_4}\dots\rho_{B_6})$.
 - 7: Perform optimization of $\mathcal{F}_2(\theta) = \sum_{k=1}^3 L_k - \beta^{-1}C_0$ and update parameters of θ ;
 - 8: Repeat 3-7 until the loss function $\mathcal{F}_2(\theta)$ converges with tolerance ε ;
 - 9: Output the state $\rho^{out} = \text{Tr}_A U(\theta)|00\rangle\langle 00|_{AB}U(\theta)^\dagger$.
-

In particular, Algorithm 1 can be efficiently implemented on near-term quantum devices since the estimation of loss function \mathcal{F}_2 only requires measuring the expected value $\langle H \rangle_\rho$ and the purity or the state overlap $\text{Tr} \rho^2$. To compute the state overlap, one approach is to utilize the well-known Swap test [42, 43], which has a simple physical implementation in quantum optics [44, 45] and can be experimentally implemented on near-term quantum hardware [30, 46, 47].

In this paper, we use a variant version of the Swap test (see Fig. 2), named destructive Swap test [48, 49]. Compared to the general Swap test, destructive Swap test is more practical on near term devices, since it is ancilla-free and costs less circuit depth and the number of the gates. As for the computation of higher order state overlaps, e.g., $\text{Tr}(\rho^3)$, there are methods using the similar circuit to that of the destructive Swap test [50], whose depth is only 2. In this paper, we call this method the higher order state overlap estimation. For more information, please refer to [50].

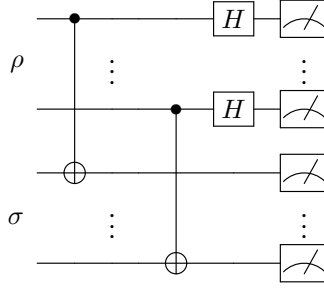


FIG. 2: Quantum circuit for implementing Destructive Swap Test

B. Performance analysis of our method

In this section, we analyze the performance of our variational algorithm. We first define a formal optimization problem that aims to find the global minimum of the loss function. Second, we give an upper bound on the difference between the von Neumann entropy $S(\rho)$ and its K -truncated version $S_K(\rho)$, which ensures the quality of Gibbs state preparation via our loss function.

a. Loss function In our algorithm (Algorithm 2), the K -truncated-free energy \mathcal{F}_K is taken as the loss function. In the optimization loop, parameters θ are updated via minimizing the loss function, and the optimization iterates until termination condition is reached. After obtaining the optimal parameters θ_{opt} , an approximation operator for the quantum Gibbs state can be prepared by performing the ansatz or parameterized circuit $U(\theta)$ with parameters θ_{opt} .

Let $K \in \mathbb{Z}_+$ be a positive integer, and truncate the von Neumann entropy $S_K(\rho)$ at order K . Hence, the K -truncated entropy $S_K(\rho)$ is given as follows,

$$S_K(\rho) = \sum_{k=1}^K \frac{(-1)^k}{k} \text{Tr} \left((\rho - I)^k \rho \right) = \sum_{j=0}^K C_j \text{Tr}(\rho^{j+1}). \quad (5)$$

Coefficients C_j 's of $S_K(\rho)$ in Eq. (5) are given in the form below,

$$C_0 = \sum_{k=1}^K \frac{1}{k}, \quad C_j = \sum_{k=j}^K \binom{k}{j} \frac{(-1)^j}{k} \quad (\forall j \in \{1, \dots, K-1\}), \quad C_K = \frac{(-1)^K}{K}. \quad (6)$$

Let H denote the Hamiltonian and $\beta > 0$ be the inverse temperature, then the loss function $\mathcal{F}_K(\theta)$ is defined as

$$\mathcal{F}_K(\theta) = \text{Tr}(H\rho(\theta)) - \beta^{-1}S_K(\rho(\theta)). \quad (7)$$

Our goal is to find parameters θ_{opt} that minimize the value of the loss function $\mathcal{F}_K(\theta)$, i.e., $\theta_{opt} = \text{argmin}_{\theta} \mathcal{F}_K(\theta)$. Note that the optimization loop only terminates if some condition given previously is reached. Therefore, one cannot obtain the true optimum but some parameters θ_0 that will approximately minimize the loss function in the sense that

$$\mathcal{F}_K(\theta_0) \leq \min_{\theta} \mathcal{F}_K(\theta) + \epsilon, \quad (8)$$

where ϵ is the error tolerance in the optimization problem.

b. Error analysis Since the loss function $\mathcal{F}_K(\boldsymbol{\theta})$ is a truncated version of the free energy, thus the solution $\boldsymbol{\theta}_0$ to the optimization problem in Eq. (8) cannot directly be used to prepare the quantum Gibbs state ρ_G . However, the obtained state $\rho(\boldsymbol{\theta}_0)$ is not far away from the Gibbs state ρ_G , where the distance is measured in terms of fidelity. In the following, we show the validity of this claim by providing a lower bound on the fidelity between $\rho(\boldsymbol{\theta}_0)$ and ρ_G .

Theorem 1 *Given a positive integer K and error tolerance $\epsilon > 0$, let $\beta > 0$ be the inverse temperature, and $\boldsymbol{\theta}_0$ be the solution to the optimization in Eq. (8). Assume the rank of the output state $\rho(\boldsymbol{\theta}_0)$ is r , then the fidelity between the state $\rho(\boldsymbol{\theta}_0)$ and the Gibbs state ρ_G is lower bounded as follows*

$$F(\rho(\boldsymbol{\theta}_0), \rho_G) \geq 1 - \sqrt{2\beta \left(\epsilon + \frac{2r}{K+1} (1-\Delta)^{K+1} \right)}, \quad (9)$$

where $\Delta \in (0, e^{-1})$ is a constant determined by K .

Theorem 1 implies that we can regard the output state $\rho(\boldsymbol{\theta}_0)$ as an approximation for the Gibbs state for a given error tolerance in the optimization problem and a truncation order K . And quantity in Eq. (9) quantifies how much $\rho(\boldsymbol{\theta}_0)$ approximates ρ_G .

In the following, we prove Theorem 1 by building a connection between the relative entropy and the fidelity, and deriving an upper bound on the truncation error.

Lemma 2 *Given quantum states ρ and σ and a constant $\delta > 0$, suppose that the relative entropy $S(\rho||\sigma)$ is less than δ , i.e., $S(\rho||\sigma) \leq \delta$. Then the fidelity between ρ and σ is lower bounded. To be specific, $F(\rho, \sigma) \geq 1 - \sqrt{2\delta}$.*

Proof Recall the relationship between the trace distance and the fidelity $D(\rho, \sigma) \geq 1 - F(\rho, \sigma)$, and Pinsker's inequality $D(\rho, \sigma) \leq \sqrt{2S(\rho||\sigma)}$, then we have the following inequality,

$$F(\rho, \sigma) \geq 1 - D(\rho, \sigma) \geq 1 - \sqrt{2S(\rho||\sigma)} \geq 1 - \sqrt{2\delta}. \quad (10)$$

■

Lemma 2 states that, if one wants to lower bound the fidelity $F(\rho(\boldsymbol{\theta}_0), \rho_G)$ between the obtained state $\rho(\boldsymbol{\theta}_0)$ and the Gibbs state ρ_G , then one only needs to upper bound the relative entropy $S(\rho(\boldsymbol{\theta}_0)||\rho_G)$ between them.

Next, we proceed to give an upper bound of the relative entropy.

Let δ_0 be the truncation error of $S_K(\rho)$, then the definition of the free energy allows to bound the difference between the free energy and its truncated version, i.e., $|\mathcal{F}_K(\rho) - \mathcal{F}(\rho)| \leq \delta_0$. Recalling the well-known free energy equality, $\mathcal{F}(\rho) = \mathcal{F}(\rho_G) + \beta^{-1}S(\rho||\rho_G)$, this equality states that, for arbitrary density ρ , the free energy $\mathcal{F}(\rho)$ can be represented as a linear combination of the free energy $\mathcal{F}(\rho_G)$ of the quantum Gibbs state and the relative entropy between ρ and ρ_G . Therefore, an upper bound of the relative entropy $S(\rho(\boldsymbol{\theta}_0)||\rho_G)$ is derived as follows.

$$S(\rho(\boldsymbol{\theta}_0)||\rho_G) = \beta|\mathcal{F}(\rho(\boldsymbol{\theta}_0)) - \mathcal{F}(\rho_G)| \quad (11)$$

$$= \beta|\mathcal{F}(\rho(\boldsymbol{\theta}_0)) - \mathcal{F}_K(\rho(\boldsymbol{\theta}_0)) + \mathcal{F}_K(\rho(\boldsymbol{\theta}_0)) - \mathcal{F}(\rho_G)| \quad (12)$$

$$= \beta(\delta_0 + |\mathcal{F}_K(\rho(\boldsymbol{\theta}_0)) - \mathcal{F}(\rho_G)|) \quad (13)$$

$$\leq \beta(2\delta_0 + \epsilon), \quad (14)$$

where the inequality in Eq. (14) is due to the fact that $\mathcal{F}(\rho_G) \leq \mathcal{F}_K(\rho(\boldsymbol{\theta}_0)) \leq \mathcal{F}(\rho_G) + \delta_0 + \epsilon$ (c.f. Lemma S1 in Appendix II A).

Recall in Eq. (5) the definition of the truncated entropy $S_K(\rho)$, and notice that the truncation error of $S_K(\rho)$ is also the truncation error of loss function $\mathcal{F}_K(\rho)$. Given the truncation order K , we derive an upper bound on the difference between $S_K(\rho)$ and $S(\rho)$ in the following lemma.

Lemma 3 Given a quantum state ρ , assume the truncation order of the truncated von Neumann entropy is $K \in \mathbb{Z}_+$, and choose $\Delta \in (0, e^{-1})$ such that $-\Delta \ln(\Delta) < \frac{1}{K+1}(1-\Delta)^{K+1}$. Let δ_0 denote the truncation error, i.e., the difference between the von Neumann entropy $S(\rho)$ and its K -truncated entropy $S_K(\rho)$. Then the truncated error δ_0 is upper bounded in the sense that

$$\delta_0 \leq \frac{r}{K+1} (1-\Delta)^{K+1}, \quad (15)$$

where r denotes the rank of density operator.

Proof The proof proceeds by expanding the logarithm function in the entropy into Taylor series. The upper bound of the difference between the entropy $S(\rho)$ and its truncated version $S_K(\rho)$ for density ρ is given as follows,

$$\delta_0 = |S(\rho) - S_K(\rho)| \quad (16)$$

$$= \left| \text{Tr} \left(\sum_{k=K+1}^{\infty} \frac{(-1)^k}{k} (\rho - I)^k \rho \right) \right| \quad (17)$$

$$= \sum_{j: \lambda_j \geq \Delta} \lambda_j \sum_{k=K+1}^{\infty} \frac{1}{k} (1-\lambda_j)^k + \sum_{j: 0 < \lambda_j < \Delta} \lambda_j \sum_{k=K+1}^{\infty} \frac{1}{k} (1-\lambda_j)^k. \quad (18)$$

In the above Eq. (18) we use the spectral decomposition of $\rho = \sum_{j=1}^r \lambda_j |\psi_j\rangle\langle\psi_j|$.

To give an upper bound on truncation error δ_0 , we give upper bounds on two terms in Eq. (18). First, we consider the term with eigenvalues larger than Δ .

$$\sum_{j: \lambda_j \geq \Delta} \lambda_j \sum_{k=K+1}^{\infty} \frac{1}{k} (1-\lambda_j)^k = \sum_{j: \lambda_j \geq \Delta} \sum_{k=K+1}^{\infty} \frac{1}{k} (1-\lambda_j)^k - \sum_{j: \lambda_j \geq \Delta} \sum_{k=K+1}^{\infty} \frac{1}{k} (1-\lambda_j)^{k+1} \quad (19)$$

$$\leq \sum_{j: \lambda_j \geq \Delta} \sum_{k=K+1}^{\infty} \frac{1}{k} (1-\lambda_j)^k - \sum_{j: \lambda_j \geq \Delta} \sum_{k=K+1}^{\infty} \frac{1}{k+1} (1-\lambda_j)^{k+1} \quad (20)$$

$$= \frac{1}{K+1} \sum_{j: \lambda_j \geq \Delta} (1-\lambda_j)^{K+1}. \quad (21)$$

The equality in Eq. (19) is due to the substitution of λ_j with $1 - (1 - \lambda_j)$, and the inequality in (20) follows by replacing $1/k$ with $1/(k+1)$ in the right summation of Eq. (19).

Then we consider the term with non-zero eigenvalues less than Δ .

$$\sum_{j: 0 < \lambda_j < \Delta} \lambda_j \sum_{k=K+1}^{\infty} \frac{1}{k} (1-\lambda_j)^k \leq \sum_{j: 0 < \lambda_j < \Delta} -\lambda_j \ln(\lambda_j) \quad (22)$$

$$\leq \sum_{j: 0 < \lambda_j < \Delta} -\Delta \ln(\Delta), \quad (23)$$

where the inequality in Eq. (22) follows from replacing the series with $-\ln(\lambda_j)$, since function $S(x) = -x \ln(x) = \sum_{l=1}^{\infty} \frac{1}{l} x(1-x)^l$, and the second inequality is due to the fact that $S(x)$ increases as x increases in the interval $(0, e^{-1})$.

In all, an upper bound on δ_0 can be given as

$$\delta_0 \leq \frac{1}{K+1} \sum_{j: \lambda_j \geq \Delta} (1-\lambda_j)^{K+1} + \sum_{j: 0 < \lambda_j < \Delta} -\Delta \ln(\Delta) \quad (24)$$

$$\leq r \cdot \left(\frac{r_0 (1 - \Delta)^{K+1}}{r (K + 1)} + \frac{r_1}{r} (-\Delta \ln(\Delta)) \right) \quad (25)$$

$$\leq r \cdot \max\left\{ \frac{(1 - \Delta)^{K+1}}{K + 1}, -\Delta \ln(\Delta) \right\}. \quad (26)$$

where r_0 (r_1) denotes the number of non-zero eigenvalues larger (less) than Δ . As $-\Delta \ln(\Delta) < \frac{1}{K+1}(1 - \Delta)^{K+1}$, the claim is proved. ■

Replacing δ_0 in Eq. (14) with its upper bound in Eq. (15) immediately obtains a bound on the relative entropy $S(\rho(\boldsymbol{\theta}_0) \parallel \rho_G)$. Taking this bound into Lemma 2, a lower bound on the fidelity $F(\rho(\boldsymbol{\theta}), \rho_G)$ is derived, which is exactly the one in Eq. (9), and the proof of Theorem 1 is completed.

C. Optimization via the gradient-based method

Finding optimal parameters $\boldsymbol{\theta}_{opt}$ is a major part of our variational algorithm. Both gradient-based and gradient-free methods could be used to do the optimization. Here, we provide analytical details on the gradient-based approach and we refer to [36] for more information on the optimization subroutines in variational quantum algorithms. As the evaluation of higher order truncations may be too costly for NISQ devices with limited circuit width, we mainly focus on the 2-truncated free energy $\mathcal{F}_2(\boldsymbol{\theta})$ and choose it as our loss function. In particular, we show that this loss function is convex, which indicates that gradient-based method could work efficiently on minimizing the loss function. We further derive the analytical expressions for its gradients and show that these analytical gradients could also be evaluated efficiently on NISQ devices.

In the following, we first give a proof for the convexity of $\mathcal{F}_2(\rho)$, and then derive explicit expressions of the gradients of the loss function and show that the same circuit used to compute the loss function can be used to calculate their gradients.

a. Convexity of 2-truncated free energy Recall the definition of K -truncated entropy $S_K(\rho)$ in Eq. (5), and, in this section, we take $K = 2$. Given truncation order 2, the loss function $\mathcal{F}_2(\rho)$ is defined in the following form,

$$\mathcal{F}_2(\boldsymbol{\theta}) = \text{Tr}(H\rho(\boldsymbol{\theta})) + \beta^{-1} \left(2 \text{Tr}(\rho(\boldsymbol{\theta})^2) - \frac{1}{2} \text{Tr}(\rho(\boldsymbol{\theta})^3) - \frac{3}{2} \right). \quad (27)$$

Notice that the functional $\text{Tr}(H\rho)$ is linear for a given Hamiltonian H and $\beta > 0$, therefore the convexity of loss function \mathcal{F}_2 is determined by the convexity of the functional $g(\rho) = 2 \text{Tr}(\rho^2) - \frac{1}{2} \text{Tr}(\rho^3) - \frac{3}{2}$. Hence, to prove the convexity of \mathcal{F}_2 , we only need to show the convexity of functional $g(\rho)$.

Lemma 4 *The functional $g(\rho) = 2 \text{Tr}(\rho^2) - \frac{1}{2} \text{Tr}(\rho^3) - \frac{3}{2}$ is convex, where ρ is a density operator.*

Proof According to Theorem 2.10 of [51], the functional $\text{Tr}(f(\rho))$ is convex if the associated function $f : \mathbb{R} \rightarrow \mathbb{R}$ is convex. In the scenario, where $\mathcal{F}_2(\rho)$ is given in Eq. (27), the associated function of g is defined as $f(x) = 2x^2 - \frac{1}{2}x^3 - \frac{3}{2}$ for all $x \in [0, 1]$. The claim follows from proving that f is convex, and the second order derivative $f^{(2)}$ of f is positive, since

$$f^{(2)}(x) = 4 - 3x \geq 1 \quad \forall x \in [0, 1]. \quad (28)$$

Therefore, the positivity of the second order derivative of f leads to the convexity of $\mathcal{F}_2(\rho)$ in the set of densities operators. ■

b. Analytical gradient Here we discuss the computation of the gradient of the global loss function $\mathcal{F}_2(\boldsymbol{\theta})$. Inspired by previous works [52–54], we compute the gradients of the 2-truncated free energy \mathcal{F}_2 by shifting the parameters of the same circuit for estimating \mathcal{F}_2 . Note that there is an alternative method to estimate the partial derivative with a single circuit [55], but at the cost of using an ancillary qubit.

In Fig. 1, the density operator $\rho(\boldsymbol{\theta})$ is prepared in the register B by performing a sequence of unitaries $U = U_N \dots U_1$ on the state $|00\rangle_{AB}$ in registers AB , and then measuring in register A . Each gate U_m is either fixed, e.g., a C-NOT gate, or parameterized. The parameterized gates are of the form $U_m = e^{-iH_m\theta_m/2}$, where θ_m 's are real parameters and H_m 's are a tensor product of Pauli matrices. Then the loss function \mathcal{F}_2 is related to parameters $\boldsymbol{\theta}$, and its gradient is explicitly given by

$$\nabla_{\boldsymbol{\theta}} \mathcal{F}_2(\boldsymbol{\theta}) = \left(\frac{\partial \mathcal{F}_2(\boldsymbol{\theta})}{\partial \theta_1}, \dots, \frac{\partial \mathcal{F}_2(\boldsymbol{\theta})}{\partial \theta_N} \right). \quad (29)$$

Particularly, the partial derivatives of \mathcal{F}_2 with respect to θ_m is

$$\begin{aligned} \frac{\partial \mathcal{F}_2(\boldsymbol{\theta})}{\partial \theta_m} = & \frac{1}{2} (\langle K \rangle_{\theta_m + \frac{\pi}{2}} - \langle K \rangle_{\theta_m - \frac{\pi}{2}}) + \\ & \beta^{-1} [(2(\langle O \rangle_{\theta_m + \frac{\pi}{2}, \theta_m} - \langle O \rangle_{\theta_m - \frac{\pi}{2}, \theta_m}) - \frac{3}{4} (\langle G \rangle_{\theta_m + \frac{\pi}{2}, \theta_m, \theta_m} - \langle G \rangle_{\theta_m - \frac{\pi}{2}, \theta_m, \theta_m})], \end{aligned} \quad (30)$$

where $\langle K \rangle$, $\langle O \rangle$, and $\langle G \rangle$ are used to estimate $\text{Tr}(H\rho(\boldsymbol{\theta}))$, $\text{Tr}(\rho(\boldsymbol{\theta})^2)$, and $\text{Tr}(\rho(\boldsymbol{\theta})^3)$, respectively. The definitions of $\langle K \rangle$, $\langle O \rangle$, and $\langle G \rangle$ are given in Eqs. (46)-(48).

To simplify the notations, let L_1 denote $\text{Tr}(H\rho(\boldsymbol{\theta}))$, L_2 denote $2\beta^{-1} \text{Tr}(\rho(\boldsymbol{\theta})^2)$, and L_3 denote $-\frac{\beta^{-1}}{2} \text{Tr}(\rho(\boldsymbol{\theta})^3)$. Using these notations, our loss function can be rewritten as $\mathcal{F}_2(\boldsymbol{\theta}) = L_1 + L_2 + L_3 - \frac{3\beta^{-1}}{2}$, and the gradient of $\mathcal{F}_2(\boldsymbol{\theta})$ can be rewritten as follow,

$$\nabla_{\boldsymbol{\theta}} \mathcal{F}_2(\boldsymbol{\theta}) = \nabla_{\boldsymbol{\theta}} L_1 + \nabla_{\boldsymbol{\theta}} L_2 + \nabla_{\boldsymbol{\theta}} L_3. \quad (31)$$

Therefore, the gradient of $\mathcal{F}_K(\boldsymbol{\theta})$ can be estimated via computing the gradients of L_j , $j = 1, 2, 3$. Specifically, $\nabla_{\boldsymbol{\theta}} L_j$, $j = 2, 3$, can be computed using the destructive SWAP test and higher order state overlap estimation, respectively. As for $\nabla_{\boldsymbol{\theta}} L_1$, it can be estimated by measurement directly.

Next, we show that the gradients of L_j 's can be computed by shifting the parameters $\boldsymbol{\theta}$ of the circuit. The partial derivatives of each L_j have the following forms,

$$\frac{\partial L_1}{\partial \theta_m} = \frac{\partial}{\partial \theta_m} \text{Tr}(U_N \dots U_m(\theta_m) \dots U_1 |0\rangle \langle 0| U_1^\dagger \dots U_m^\dagger(\theta_m) \dots U_N^\dagger \cdot (I \otimes H)), \quad (32)$$

$$\frac{\partial L_2}{\partial \theta_m} = \frac{\partial}{\partial \theta_m} \text{Tr}((U_N \dots U_m(\theta_m) \dots U_1 |0\rangle \langle 0| U_1^\dagger \dots U_m^\dagger(\theta_m) \dots U_N^\dagger)^{\otimes 2} \cdot W_1), \quad (33)$$

$$\frac{\partial L_3}{\partial \theta_m} = \frac{\partial}{\partial \theta_m} \text{Tr}((U_N \dots U_m(\theta_m) \dots U_1 |0\rangle \langle 0| U_1^\dagger \dots U_m^\dagger(\theta_m) \dots U_N^\dagger)^{\otimes 3} \cdot W_2), \quad (34)$$

where W_1 denotes the operator $\text{SWAP}_{B_2 B_3} \otimes I_{A_2 A_3}$, W_2 denotes the operator $(\text{SWAP}_{B_4 B_5} \otimes I_{A_4 A_5 A_6 B_6}) \cdot (\text{SWAP}_{B_5 B_6} \otimes I_{A_4 B_4 A_5 A_6})$, and the operator $\text{SWAP}_{B_j B_l}$ is a swap operator acting on registers B_j and B_l .

To further simplify notations, we absorb all gates before and after U_m into the density operator and measurement operator, respectively. To be more specific, let $\psi_{A_l B_l}$ denote the density operator $U_{m-1} \dots U_1 |00\rangle \langle 00|_{A_l B_l} U_1^\dagger \dots U_{m-1}^\dagger$ in register $A_l B_l$, for $l = 1, \dots, 6$. And we define observable operators K, O, G as follows

$$K = U_{m+1}^\dagger \dots U_N^\dagger (I_{A_1} \otimes H_{B_1}) U_N \dots U_{m+1}. \quad (35)$$

$$O = (U_{m+1}^\dagger \dots U_N^\dagger)^{\otimes 2} W_1 (U_N \dots U_{m+1})^{\otimes 2}, \quad (36)$$

$$G = (U_{m+1}^\dagger \dots U_N^\dagger)^{\otimes 3} W_2 (U_N \dots U_{m+1})^{\otimes 3}. \quad (37)$$

Then partial derivatives in Eqs. (32)-(34) can be rewritten as

$$\frac{\partial L_1}{\partial \theta_m} = \frac{\partial}{\partial \theta_m} \text{Tr}(U_m(\theta_m) \psi_{A_1 B_1} U_m^\dagger(\theta_m) \cdot K), \quad (38)$$

$$\frac{\partial L_2}{\partial \theta_m} = \frac{\partial}{\partial \theta_m} \text{Tr}(U_m \psi_{A_2 B_2} U_m^\dagger(\theta_m) \otimes U_m \psi_{A_3 B_3} U_m^\dagger(\theta_m) \cdot O), \quad (39)$$

$$\frac{\partial L_3}{\partial \theta_m} = \frac{\partial}{\partial \theta_m} \text{Tr}(U_m \psi_{A_4 B_4} U_m^\dagger(\theta_m) \otimes U_m \psi_{A_5 B_5} U_m^\dagger(\theta_m) \otimes U_m \psi_{A_6 B_6} U_m^\dagger(\theta_m) \cdot G). \quad (40)$$

Now, we derive the analytical forms of the derivatives of each L_j , $j = 1, 2, 3$. Notice that the trainable unitary $U(\boldsymbol{\theta})$ is a sequence of unitaries $U_m(\theta_m)$ and each unitary $U_m(\theta_m) = e^{-i\theta_m H_m/2}$. The partial derivative of $U(\boldsymbol{\theta})$ can be explicitly given as follows,

$$\frac{\partial U(\boldsymbol{\theta})}{\partial \theta_m} = U_N(\theta_N) \dots \frac{\partial U_m(\theta_m)}{\partial \theta_m} \dots U_1(\theta_1), \quad (41)$$

$$= -\frac{i}{2} U_N(\theta_N) \dots H_m U_m \dots U_1(\theta_1). \quad (42)$$

Using the expression of $\partial_{\theta_m} U(\boldsymbol{\theta})$ in Eq. (42), and some facts, including an identity $i[H_m, M] = U_m(-\pi/2) M U_m^\dagger(-\pi/2) - U_m(\pi/2) M U_m^\dagger(\pi/2)$, which holds true for arbitrary matrix M , the symmetry of the operator O , and an equality $\partial_{\theta_m} \text{Tr}(\rho(\boldsymbol{\theta})^3) = 3\partial_{\theta_{m1}} \text{Tr}(\rho_1(\boldsymbol{\theta}) \otimes \rho_2(\boldsymbol{\theta}) \otimes \rho_3(\boldsymbol{\theta}) \cdot S_1 S_2)$ (c.f. Lemma S2 in Appendix II B), where $S_1 = \text{SWAP}_{12} \otimes I_3$ and $S_2 = I_1 \otimes \text{SWAP}_{23}$, the gradients of each L_j can be estimated using the following formulas,

$$\frac{\partial L_1}{\partial \theta_m} = \frac{1}{2} (\langle K \rangle_{\theta_m + \frac{\pi}{2}} - \langle K \rangle_{\theta_m - \frac{\pi}{2}}), \quad (43)$$

$$\frac{\partial L_2}{\partial \theta_m} = \langle O \rangle_{\theta_m + \frac{\pi}{2}, \theta_m} - \langle O \rangle_{\theta_m - \frac{\pi}{2}, \theta_m}, \quad (44)$$

$$\frac{\partial L_3}{\partial \theta_m} = \frac{3}{2} (\langle G \rangle_{\theta_m + \frac{\pi}{2}, \theta_m, \theta_m} - \langle G \rangle_{\theta_m - \frac{\pi}{2}, \theta_m, \theta_m}), \quad (45)$$

where the notation $\langle X \rangle_{a,b}$ is defined below,

$$\langle K \rangle_{\theta_\alpha} = \text{Tr}(U_\alpha \psi_{A_1 B_1} U_\alpha^\dagger \cdot K), \quad (46)$$

$$\langle O \rangle_{\theta_\alpha, \theta_\beta} = \text{Tr} \left(U_\alpha \psi_{A_2 B_2} U_\alpha^\dagger \otimes U_\beta \psi_{A_3 B_3} U_\beta^\dagger \cdot O \right), \quad (47)$$

$$\langle G \rangle_{\theta_\alpha, \theta_\beta, \theta_\gamma} = \text{Tr} \left(U_\alpha \psi_{A_4 B_4} U_\alpha^\dagger \otimes U_\beta \psi_{A_5 B_5} U_\beta^\dagger \otimes U_\gamma \psi_{A_6 B_6} U_\gamma^\dagger \cdot G \right). \quad (48)$$

To summarize, the above results entail that the partial derivatives of our loss function $\mathcal{F}_2(\boldsymbol{\theta})$ with respect to $\boldsymbol{\theta}$ are completely determined by Eq. (30). This indicates that the analytical gradient of our loss function $\mathcal{F}_2(\boldsymbol{\theta})$ can be efficiently computed on near-term quantum devices by shifting parameters and performing measurements. With the analytical gradients, one could apply the gradient-based methods to minimize the loss function. Specifically, parameters $\boldsymbol{\theta}$ in the unitary $U(\boldsymbol{\theta})$ are updated towards the steepest direction of the loss function, i.e.,

$$\boldsymbol{\theta} \leftarrow \boldsymbol{\theta} - \eta \nabla_{\boldsymbol{\theta}} \mathcal{F}_2(\boldsymbol{\theta}), \quad (49)$$

where $\nabla_{\boldsymbol{\theta}} \mathcal{F}_2(\boldsymbol{\theta})$ is the gradient vector and η is the learning rate that determines the step sizes. Under suitable assumptions, the loss functions converge to the global minimum after certain iterations of the above procedure. Notice that other gradient-based methods, e.g., stochastic gradient descent, ADAM [41], can also be used in the optimization loop of our variational Gibbs state preparation algorithm.

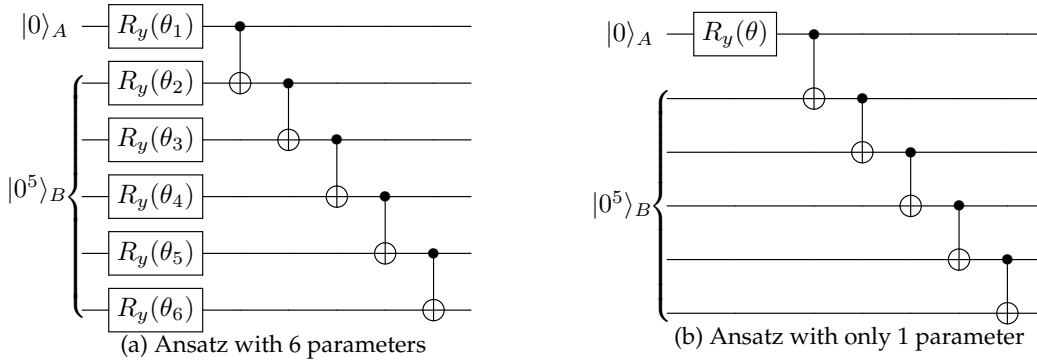


FIG. 3: Two ansatzes for Ising chain model.

III. NUMERICAL SIMULATIONS

In this section, we have conducted numerical experiments preparing the Gibbs states of two common Hamiltonian examples: Ising chain model and XY spin-1/2 chain model. In subsection III A, we study the Ising chain model and show that a parameterized circuit with one ancillary qubit and shallow depth could be trained to produce the Ising Gibbs state with fidelity higher than 99%, especially in higher β or lower temperature ($\beta \geq 2$). Furthermore, we also give a more sophisticated ansatz with only one parameter can do the same thing. As the second example, in subsection III B, we study the spin chain model and show that our approach could achieve a fidelity higher than 95% via an ansatz with 30 parameters for $\beta \geq 1.5$ for a 5-length XY spin-1/2 chain Hamiltonian. In particular, the fidelity could also achieve 99% for the lower temperature case. In our numerical experiments, the classical parameters of in the parameterized circuits are initialized from a uniform distribution in $[0, 2\pi]$, and then updated via the ADAM gradient-based method [41] until the loss function is converged. All simulations are implemented via Paddle Quantum [56] on the PaddlePaddle Deep Learning Platform [57, 58].

A. Ising model

As our first example, we consider the spin 1/2 chain B of length $L = 5$, with the Ising Hamiltonian

$$H_B = - \sum_{i=1}^L Z_{B,i} Z_{B,i+1} \quad (50)$$

and periodic boundary conditions (i.e., $Z_{B,6} = Z_{B,1}$).

Our goal is to prepare the corresponding Gibbs state

$$\rho_G = e^{-\beta H_B} / \text{Tr}(e^{-\beta H_B}). \quad (51)$$

To prepare this state, we choose a 6-qubit parametrized circuit with $n_A = 1$ and $n_B = 5$ (cf. Fig. 3), where A is the ancillary system that used for producing a mixed state on system B . Here we need to note that we only use a 1-qubit ancillary system in our ansatz, which is significantly less than [29] where $n_A = n_B$. In Fig. 3(a), the ansatz consists of 6 single qubit Pauli-Y rotation operators with different classic parameters θ_i ($i \in [6]$) and 5 CNOT gates.

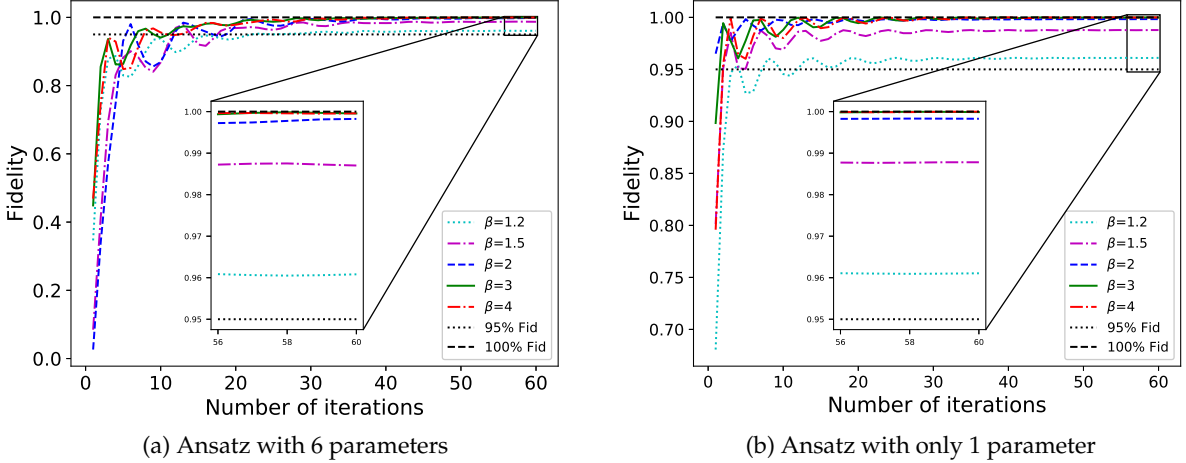


FIG. 4: Fidelity curves for the Ising chain Gibbs state preparation with different β .

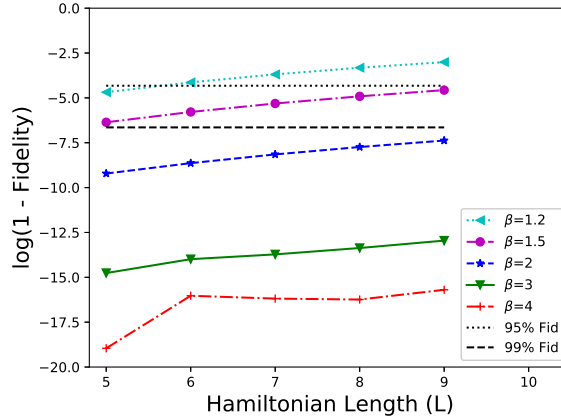


FIG. 5: Semilog plot of the fidelity vs. the Ising Hamiltonian length (L) with different β for the Ising chain model.

After applying this ansatz on the input zero state $|0\rangle_A|0^5\rangle_B$, we can get the output state on system B, which is desired to get close to the Gibbs state in Eq. (51). The fidelity between this output state and the Gibbs state, in the training process with different β , is depicted in Fig. 4(a). When $\beta \geq 1.2$, after 30 iterations of updating parameters, our method can easily achieve a fidelity higher than 95%. Specifically, if $\beta \geq 2$, the fidelity is higher than 99%, which indicates that our approach can almost exactly prepare the Gibbs state in Eq. (51), especially in higher inverse temperatures.

We also test the preparation of the Ising Gibbs state for different length (i.e., $L = 5, 6, 7, 8, 9$) and all of the ansatzes are similar to Fig. 3(a), which only uses one additional qubit. The curves of the logarithmic form of the fidelity between the output state ρ_B and the Gibbs state ρ_G are depicted in Fig. 5. We can intuitively see that the larger the Hamiltonian length is, the lower fidelity we achieve. However, we can also find that the temperature has a significant impact on fidelity: the larger the β is, the higher the fidelity is (see Proposition 6 for a detailed analysis). In particular, when $\beta \geq 2$, the fidelity is already higher than 99%, for the Hamiltonian length we have listed in the figure.

There is an interesting experimental phenomenon in the training process that the first parameter θ_1 in system A is approaching $\pi/2$ while other parameters in system B is approaching 0. Hence, we update the ansatz to a simplified one in Fig. 3(b) and implement the numerical simulations in 4(b). Notably, the overall performance is almost the same as the one using the ansatz with 6 parameters (cf. Fig. 4(a)). To further explore this interesting behaviour of the Ising chain Gibbs state preparation, we analyze the states generated by using different loss functions.

Proposition 5 *Given the circuit in Fig. 3(b) and denote $\rho_B(\theta)$ its output state on system B . For the Ising chain model, if we compute its free energy in Eq. (3) and our truncated cost in Eq. (7), then the optimal parameters that minimize these two loss functions are both*

$$\theta = \pi/2 + k\pi, \quad (52)$$

where $k \in \mathbb{Z}$. As a result, $\rho_B(\pi/2)$ is the best state, under this circuit, that approaching the Gibbs state in Eq. (51), and their fidelity could be larger than 95% for any $\beta \geq 1.25$.

We defer the proof to Appendix II C. Here, we need to note that this fidelity is just a lower bound, actually, when $\beta = 1.2$, we have still achieved a fidelity greater than 95% for $n_B = 5$, as demonstrated in our experiments. And in Proposition 5, the number of qubits in system B is not limited to 5, instead it can be any positive integer that greater than two.

Another interesting experimental result (c.f. Fig. 5) shows that the fidelity between the Ising chain Gibbs state ρ_G and the output state ρ_B of our method increases exponentially when β increases. The result is as follows and the details can be found in Appendix II D.

Proposition 6 *Given the circuit in Fig. 3(b) and let $\rho_B(\theta)$ be its output state on system B . Then the fidelity between $\rho_B(\pi/2)$ and the Gibbs state ρ_G is lower bounded. To be more specific,*

$$F(\rho_B(\pi/2), \rho_G) \geq \frac{1}{\sqrt{1 + (N/2 - 1)e^{-\beta\Delta}}}, \quad (53)$$

where N is the dimension of system B , i.e., $N = 2^{n_B}$ and Δ is the spectral gap of the Gibbs state ρ_G , i.e., the discrepancy between the minimum and the second minimum eigenvalues.

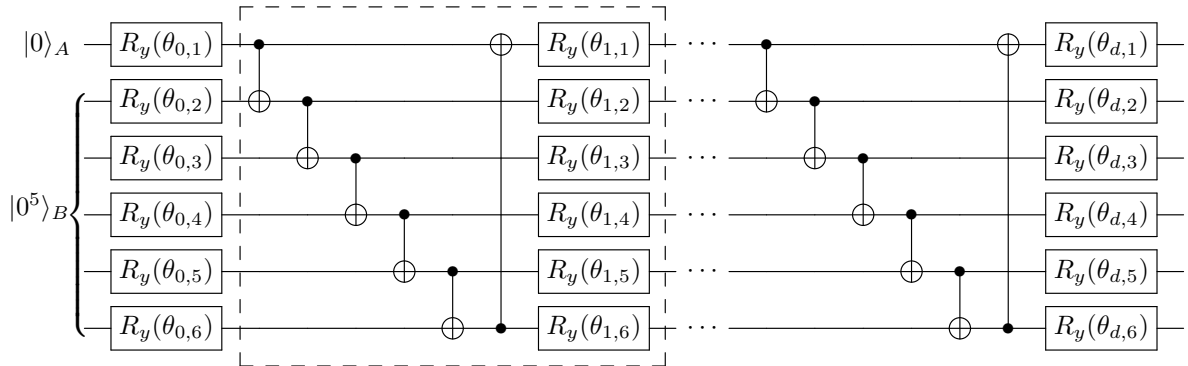


FIG. 6: The ansatz for XY spin-1/2 chain model. Here, d means repeating d times the basic circuit module (denoted in the dashed-line box).

B. XY spin-1/2 chain model

Our second instance is the XY spin-1/2 chain B of length $L = 5$, with the Hamiltonian

$$H_B = - \sum_{i=1}^L X_{B,i} X_{B,i+1} + Y_{B,i} Y_{B,i+1} \quad (54)$$

and periodic boundary conditions (i.e., $Z_{B,6} = Z_{B,1}$).

To prepare the spin chain Gibbs state, we first choose a 6-qubit parametrized circuit with $n_A = 1$ and $n_B = 5$ (cf. Fig. 6), where the basic circuit module (which contains a CNOT layer and a layer of single qubit Pauli-Y rotation operators) is repeated d times, and the total number of parameters of this circuit is $(n_A + n_B)(d + 1)$.

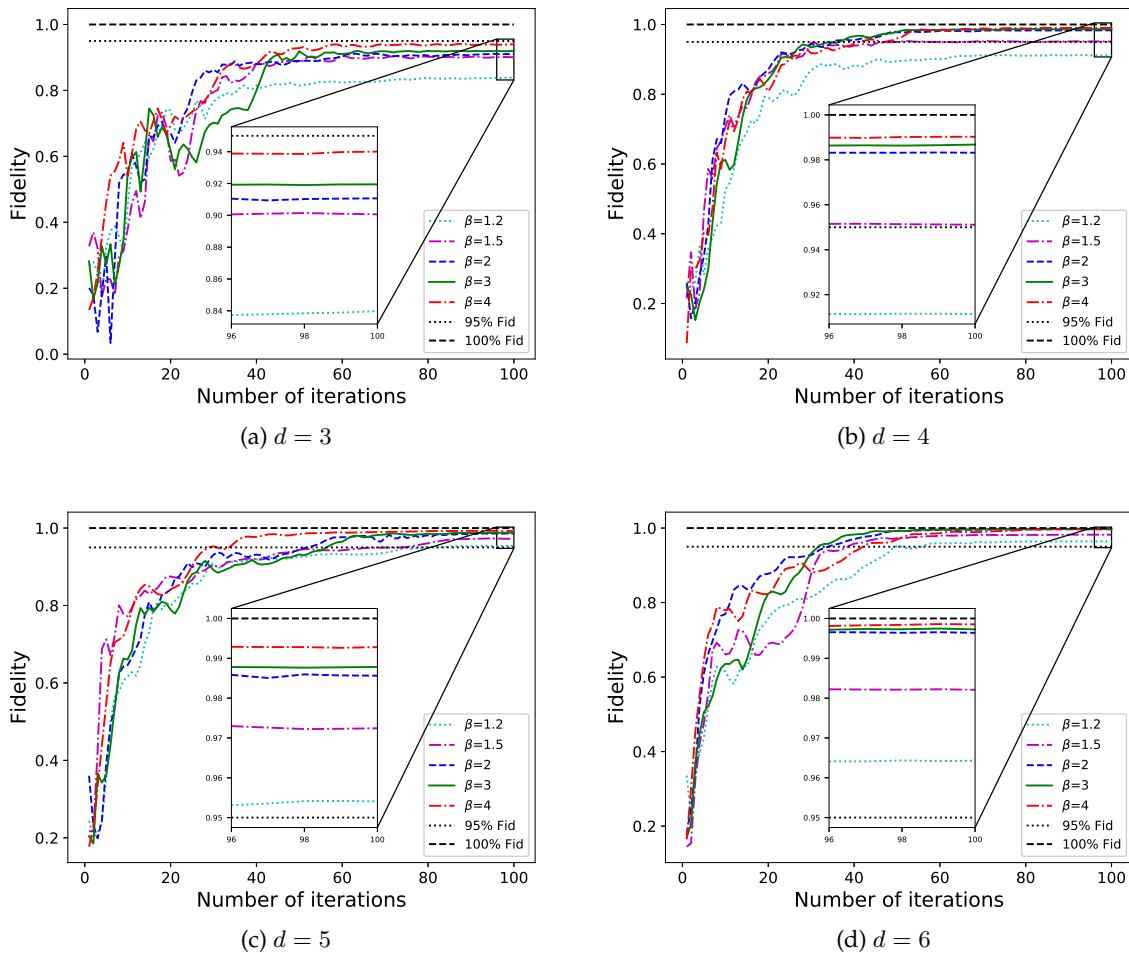


FIG. 7: Fidelity curves for the XY spin-1/2 chain Gibbs state preparation with different β . Here, each d indicates the ansatz has $(n_A + n_B)(d + 1) = 6(d + 1)$ parameters.

The fidelity between the output state of this circuit and the Gibbs state is shown in Fig. 7, where different d 's are included. We see that when $d \geq 4$ and $\beta \geq 1.5$, our approach can easily achieve a fidelity greater than 95% and if $\beta \geq 2$, the fidelity could higher than 98%. Furthermore, if β is equaling to 4, the fidelity can even higher than 99%, which means our approach could almost

generate the Gibbs state exactly in higher β (or lower temperature). One possible reason that we need larger d for this instance is that the Hamiltonian in Eq. (54) is not directly generated via the CNOT module, hence we will need multiple CNOT modules to fully entangle the state.

IV. DISCUSSIONS

In this work, we provide hardware-efficient variational algorithms for quantum Gibbs state preparation with NISQ devices. We design loss functions to approximate the free energy of a given hamiltonian by utilizing the truncated Taylor series of the von Neumann entropy. By minimizing the loss functions, the parametrized quantum circuits can be trained to learn the Gibbs state via variational algorithms since the Gibbs state minimizes free energy. In particular, we show that both the loss functions and their gradients can be evaluated on NISQ devices, thus allowing us to implement the hybrid quantum-classical optimization via either gradient-based or gradient-free optimization methods. Moreover, we show that our method could prepare the Gibbs states efficiently via both analytical evidence and numerical experiments.

We further show that our variational algorithms work efficiently for many-body models including the Ising chain and spin chain. In particular, we show that the preparation of Ising Gibbs state can be done efficiently and accurately via shallow parameterized quantum circuits with only one parameter and one additional qubit. We also expect that our results may shed light on quantum optimization, quantum simulation, and quantum machine learning in the NISQ era.

Acknowledgements

We would like to thank Runyao Duan, Yuan Feng, and Sanjiang Li for helpful discussions. Y. W. and G. L. contribute equally to this work and acknowledge support from the Baidu-UTS AI Meets Quantum project. G. L. acknowledges the financial support from China Scholarship Council (No. 201806070139). This work was partly supported by the Australian Research Council (Grant No: DP180100691).

-
- [1] A. M. Childs, D. Maslov, Y. Nam, N. J. Ross, and Y. Su, "Toward the first quantum simulation with quantum speedup," *Proceedings of the National Academy of Sciences*, vol. 115, no. 38, pp. 9456–9461, 2018. [Online]. Available: <https://www.pnas.org/content/115/38/9456.short>
 - [2] M. Kieferová and N. Wiebe, "Tomography and generative training with quantum boltzmann machines," *Physical Review A*, vol. 96, no. 6, p. 062327, 2017. [Online]. Available: <https://journals.aps.org/pr/abstract/10.1103/PhysRevA.96.062327>
 - [3] J. Biamonte, P. Wittek, N. Pancotti, P. Rebentrost, N. Wiebe, and S. Lloyd, "Quantum machine learning," *Nature*, vol. 549, no. 7671, pp. 195–202, 2017. [Online]. Available: <https://www.nature.com/articles/nature23474>
 - [4] R. D. Somma, S. Boixo, H. Barnum, and E. Knill, "Quantum simulations of classical annealing processes," *Physical review letters*, vol. 101, no. 13, p. 130504, 2008. [Online]. Available: <https://journals.aps.org/prl/abstract/10.1103/PhysRevLett.101.130504>
 - [5] —, "Quantum Simulations of Classical Annealing Processes," *Physical Review Letters*, vol. 101, no. 13, p. 130504, sep 2008. [Online]. Available: <http://dx.doi.org/10.1103/PhysRevLett.101.130504>
 - [6] F. G. Brandao and K. M. Svore, "Quantum Speed-Ups for Solving Semidefinite Programs," in *2017 IEEE 58th Annual Symposium on Foundations of Computer Science (FOCS)*. IEEE, oct 2017, pp. 415–426. [Online]. Available: <http://arxiv.org/abs/1609.05537><http://ieeexplore.ieee.org/document/8104077/>

- [7] M. Kieferová and N. Wiebe, “Tomography and generative training with quantum Boltzmann machines,” *Physical Review A*, vol. 96, no. 6, p. 062327, dec 2017. [Online]. Available: <http://dx.doi.org/10.1103/PhysRevA.96.062327>
- [8] J. Watrous, “Quantum Computational Complexity,” in *Computational Complexity*. New York, NY: Springer New York, apr 2012, vol. 9781461418, pp. 2361–2387. [Online]. Available: http://link.springer.com/10.1007/978-1-4614-1800-9_{_}147
- [9] D. Aharonov, I. Arad, and T. Vidick, “The quantum pcp conjecture,” *arXiv preprint arXiv:1309.7495*, 2013. [Online]. Available: <https://arxiv.org/abs/1309.7495>
- [10] D. Poulin and P. Wocjan, “Sampling from the Thermal Quantum Gibbs State and Evaluating Partition Functions with a Quantum Computer,” *Physical Review Letters*, vol. 103, no. 22, p. 220502, nov 2009. [Online]. Available: <https://link.aps.org/doi/10.1103/PhysRevLett.103.220502>
- [11] N. Wiebe, A. Kapoor, and K. M. Svore, “Quantum deep learning,” *Quantum Information and Computation*, vol. 16, pp. 541–587, 2016. [Online]. Available: <https://dl.acm.org/doi/abs/10.5555/3179466.3179467>
- [12] M.-H. Yung and A. Aspuru-Guzik, “A quantum-quantum Metropolis algorithm,” *Proceedings of the National Academy of Sciences*, vol. 109, no. 3, pp. 754–759, jan 2012. [Online]. Available: <http://www.pnas.org/cgi/doi/10.1073/pnas.1111758109>
- [13] D. B. Kaplan, N. Klco, and A. Roggero, “Ground States via Spectral Combing on a Quantum Computer,” *arXiv:1709.08250*, sep 2017. [Online]. Available: <http://arxiv.org/abs/1709.08250>
- [14] A. Riera, C. Gogolin, and J. Eisert, “Thermalization in Nature and on a Quantum Computer,” *Physical Review Letters*, vol. 108, no. 8, p. 080402, feb 2012. [Online]. Available: <https://link.aps.org/doi/10.1103/PhysRevLett.108.080402>
- [15] M. Motta, C. Sun, A. T. K. Tan, M. J. O’Rourke, E. Ye, A. J. Minnich, F. G. S. L. Brandão, and G. K.-L. Chan, “Determining eigenstates and thermal states on a quantum computer using quantum imaginary time evolution,” *Nature Physics*, vol. 16, no. 2, pp. 205–210, feb 2020. [Online]. Available: <http://www.nature.com/articles/s41567-019-0704-4>
- [16] E. Bilgin and S. Boixo, “Preparing Thermal States of Quantum Systems by Dimension Reduction,” *Physical Review Letters*, vol. 105, no. 17, p. 170405, oct 2010. [Online]. Available: <https://link.aps.org/doi/10.1103/PhysRevLett.105.170405>
- [17] D. Poulin and P. Wocjan, “Sampling from the thermal quantum gibbs state and evaluating partition functions with a quantum computer,” *Physical review letters*, vol. 103, no. 22, p. 220502, 2009. [Online]. Available: <https://journals.aps.org/prl/abstract/10.1103/PhysRevLett.103.220502>
- [18] M.-H. Yung and A. Aspuru-Guzik, “A quantum–quantum metropolis algorithm,” *Proceedings of the National Academy of Sciences*, vol. 109, no. 3, pp. 754–759, 2012. [Online]. Available: <https://www.pnas.org/content/109/3/754.short>
- [19] J. Van Apeldoorn, A. Gilyén, S. Gribling, and R. de Wolf, “Quantum sdp-solvers: Better upper and lower bounds,” *Quantum*, vol. 4, p. 230, 2020. [Online]. Available: <https://quantum-journal.org/papers/q-2020-02-14-230/>
- [20] J. R. McClean, J. Romero, R. Babbush, and A. Aspuru-Guzik, “The theory of variational hybrid quantum-classical algorithms,” *New Journal of Physics*, vol. 18, no. 2, p. 023023, 2016. [Online]. Available: <https://iopscience.iop.org/article/10.1088/1367-2630/18/2/023023>
- [21] X. Xu, J. Sun, S. Endo, Y. Li, S. C. Benjamin, and X. Yuan, “Variational algorithms for linear algebra,” *arXiv preprint arXiv:1909.03898*, 2019. [Online]. Available: <https://arxiv.org/abs/1909.03898>
- [22] C. Bravo-Prieto, R. LaRose, M. Cerezo, Y. Subasi, L. Cincio, and P. J. Coles, “Variational quantum linear solver: A hybrid algorithm for linear systems,” *arXiv preprint arXiv:1909.05820*, 2019. [Online]. Available: <https://arxiv.org/abs/1909.05820>
- [23] H.-Y. Huang, K. Bharti, and P. Rebentrost, “Near-term quantum algorithms for linear systems of equations,” *arXiv preprint arXiv:1909.07344*, 2019. [Online]. Available: <https://arxiv.org/abs/1909.07344>
- [24] A. Peruzzo, J. McClean, P. Shadbolt, M.-H. Yung, X.-Q. Zhou, P. J. Love, A. Aspuru-Guzik, and J. L. O’Brien, “A variational eigenvalue solver on a photonic quantum processor,” *Nature communications*, vol. 5, p. 4213, 2014. [Online]. Available: https://www.nature.com/articles/ncomms5213?source=post_page
- [25] K. M. Nakanishi, K. Mitarai, and K. Fujii, “Subspace-search variational quantum eigensolver for excited states,” *Physical Review Research*, vol. 1, no. 3, p. 033062, 2019. [Online]. Available:

- <https://journals.aps.org/prresearch/abstract/10.1103/PhysRevResearch.1.033062>
- [26] R. LaRose, A. Tikku, É. O’Neel-Judy, L. Cincio, and P. J. Coles, “Variational quantum state diagonalization,” *npj Quantum Information*, vol. 5, no. 1, pp. 1–10, 2019. [Online]. Available: <https://www.nature.com/articles/s41534-019-0167-6>
- [27] M. Cerezo, A. Poremba, L. Cincio, and P. J. Coles, “Variational quantum fidelity estimation,” *Quantum*, vol. 4, p. 248, 2020. [Online]. Available: <https://quantum-journal.org/papers/q-2020-03-26-248/>
- [28] F. Reif, *Fundamentals of statistical and thermal physics*. Waveland Press, 2009. [Online]. Available: <https://cds.cern.ch/record/105079>
- [29] J. Wu and T. H. Hsieh, “Variational Thermal Quantum Simulation via Thermofield Double States,” *Physical Review Letters*, vol. 123, no. 22, p. 220502, nov 2019. [Online]. Available: <https://link.aps.org/doi/10.1103/PhysRevLett.123.220502>
- [30] R. Islam, R. Ma, P. M. Preiss, M. E. Tai, A. Lukin, M. Rispoli, and M. Greiner, “Measuring entanglement entropy in a quantum many-body system,” 2015. [Online]. Available: <https://www.nature.com/articles/nature15750>
- [31] A. N. Chowdhury, G. H. Low, and N. Wiebe, “A Variational Quantum Algorithm for Preparing Quantum Gibbs States,” pp. 1–13, jan 2020. [Online]. Available: <http://arxiv.org/abs/2002.00055>
- [32] S. Subramanian and M.-H. Hsieh, “Quantum algorithm for estimating Renyi entropies of quantum states,” *arXiv:1908.05251*, pp. 1–12, aug 2019. [Online]. Available: <http://arxiv.org/abs/1908.05251>
- [33] T. Li and X. Wu, “Quantum Query Complexity of Entropy Estimation,” *IEEE Transactions on Information Theory*, vol. 65, no. 5, pp. 2899–2921, may 2019. [Online]. Available: <https://ieeexplore.ieee.org/document/8543818/>
- [34] G. Brassard, P. Hoyer, M. Mosca, and A. Tapp, “Quantum amplitude amplification and estimation,” 2002, pp. 53–74. [Online]. Available: <http://www.ams.org/conm/305/>
- [35] G. H. Low and I. L. Chuang, “Hamiltonian Simulation by Qubitization,” *Quantum*, vol. 3, p. 163, jul 2019. [Online]. Available: <http://dx.doi.org/10.22331/q-2019-07-12-163>
- [36] M. Benedetti, E. Lloyd, S. Sack, and M. Fiorentini, “Parameterized quantum circuits as machine learning models,” *Quantum Science and Technology*, pp. 1–18, jun 2019. [Online]. Available: <http://iopscience.iop.org/article/10.1088/2058-9565/ab4eb5><http://arxiv.org/abs/1906.07682><http://dx.doi.org/10.1088/2058-9565/ab4eb5>
- [37] G. G. Guerreschi and M. Smelyanskiy, “Practical optimization for hybrid quantum-classical algorithms,” *arXiv preprint arXiv:1701.01450*, pp. 1–25, jan 2017. [Online]. Available: <http://arxiv.org/abs/1701.01450>
- [38] G. Verdon, M. Broughton, and J. Biamonte, “A quantum algorithm to train neural networks using low-depth circuits,” *arXiv:1712.05304*, 2017. [Online]. Available: <http://arxiv.org/abs/1712.05304>
- [39] D. Wecker, M. B. Hastings, and M. Troyer, “Training a quantum optimizer,” *Physical Review A*, vol. 94, no. 2, p. 022309, aug 2016. [Online]. Available: <https://link.aps.org/doi/10.1103/PhysRevA.94.022309>
- [40] Z. Wang, S. Hadfield, Z. Jiang, and E. G. Rieffel, “Quantum approximate optimization algorithm for MaxCut: A fermionic view,” *Physical Review A*, vol. 97, no. 2, p. 022304, feb 2018. [Online]. Available: <http://dx.doi.org/10.1103/PhysRevA.97.022304>
- [41] D. P. Kingma and J. Ba, “Adam: A method for stochastic optimization,” *arXiv preprint arXiv:1412.6980*, 2014. [Online]. Available: <https://arxiv.org/abs/1412.6980>
- [42] H. Buhrman, R. Cleve, J. Watrous, and R. de Wolf, “Quantum Fingerprinting,” *Physical Review Letters*, vol. 87, no. 16, p. 167902, sep 2001. [Online]. Available: <https://link.aps.org/doi/10.1103/PhysRevLett.87.167902>
- [43] D. Gottesman and I. Chuang, “Quantum Digital Signatures,” *arXiv:quant-ph/0105032*, may 2001. [Online]. Available: <http://arxiv.org/abs/quant-ph/0105032>
- [44] A. K. Ekert, C. M. Alves, D. K. L. Oi, M. Horodecki, P. Horodecki, and L. C. Kwak, “Direct estimations of linear and nonlinear functionals of a quantum state,” *Physical review letters*, vol. 88, no. 21, p. 217901, 2002. [Online]. Available: <https://journals.aps.org/prl/abstract/10.1103/PhysRevLett.88.217901>
- [45] J. C. Garcia-Escartin and P. Chamorro-Posada, “Swap test and Hong-Ou-Mandel effect are equivalent,” *Physical Review A*, vol. 87, no. 5, p. 052330, may 2013. [Online]. Available: <http://dx.doi.org/10.1103/PhysRevA.87.052330>
- [46] R. B. Patel, J. Ho, F. Ferreyrol, T. C. Ralph, and G. J. Pryde, “A quantum Fredkin gate,” *Science advances*, vol. 2, no. 3, p. e1501531, 2016. [Online]. Available: <https://advances.sciencemag.org/>

- [content/2/3/e1501531.abstract](#)
- [47] N. M. Linke, S. Johri, C. Figgatt, K. A. Landsman, A. Y. Matsuura, and C. Monroe, “Measuring the Rényi entropy of a two-site Fermi-Hubbard model on a trapped ion quantum computer,” *Physical Review A*, vol. 98, no. 5, p. 052334, nov 2018. [Online]. Available: <https://link.aps.org/doi/10.1103/PhysRevA.98.052334>
 - [48] A. K. Ekert, C. M. Alves, D. K. Oi, M. Horodecki, P. Horodecki, and L. C. Kwek, “Direct estimations of linear and nonlinear functionals of a quantum state,” *Physical review letters*, vol. 88, no. 21, p. 217901, 2002. [Online]. Available: <https://journals.aps.org/prl/abstract/10.1103/PhysRevLett.88.217901>
 - [49] L. Cincio, Y. Subasi, A. T. Sornborger, and P. J. Coles, “Learning the quantum algorithm for state overlap,” *New Journal of Physics*, vol. 20, no. 11, p. 113022, 2018. [Online]. Available: <https://iopscience.iop.org/article/10.1088/1367-2630/aae94a/meta>
 - [50] Y. Subasi, L. Cincio, and P. J. Coles, “Entanglement spectroscopy with a depth-two quantum circuit,” *Journal of Physics A: Mathematical and Theoretical*, vol. 52, no. 4, p. 044001, 2019. [Online]. Available: <https://iopscience.iop.org/article/10.1088/1751-8121/aaf54d/meta>
 - [51] E. Carlen, “Trace inequalities and quantum entropy: an introductory course,” *Entropy and the quantum*, vol. 529, pp. 73–140, 2010. [Online]. Available: <http://www.mathphys.org/AZschool/material/AZ09-carlen.pdf>
 - [52] K. Mitarai, M. Negoro, M. Kitagawa, and K. Fujii, “Quantum circuit learning,” *Physical Review A*, vol. 98, no. 3, p. 032309, 2018. [Online]. Available: <https://journals.aps.org/prl/abstract/10.1103/PhysRevA.98.032309>
 - [53] M. Schuld, V. Bergholm, C. Gogolin, J. Izaac, and N. Killoran, “Evaluating analytic gradients on quantum hardware,” *Physical Review A*, vol. 99, no. 3, p. 032331, mar 2019. [Online]. Available: <https://link.aps.org/doi/10.1103/PhysRevA.99.032331>
 - [54] M. Ostaszewski, E. Grant, and M. Benedetti, “Quantum circuit structure learning,” *arXiv:1905.09692*, pp. 1–11, may 2019. [Online]. Available: <http://arxiv.org/abs/1905.09692>
 - [55] E. Farhi and H. Neven, “Classification with Quantum Neural Networks on Near Term Processors,” *arXiv:1802.06002*, pp. 1–21, feb 2018. [Online]. Available: <http://arxiv.org/abs/1802.06002>
 - [56] “Paddle Quantum.” [Online]. Available: <https://github.com/paddlepaddle/Quantum>
 - [57] “PaddlePaddle.” [Online]. Available: <https://github.com/paddlepaddle/paddle>
 - [58] Y. Ma, D. Yu, T. Wu, and H. Wang, “PaddlePaddle: An Open-Source Deep Learning Platform from Industrial Practice,” *Frontiers of Data and Computing*, vol. 1, no. 1, pp. 105–115, 2019. [Online]. Available: <http://www.jfdc.cnic.cn/EN/abstract/abstract2.shtml>

Appendix

I. VARIATIONAL ALGORITHM FOR GIBBS STATE PREPARATION WITH HIGHER-ORDER TRUNCATIONS

Here we present a variational algorithm for preparing the Gibbs state with K -truncated free energy. To illustrate our algorithm, we give some notations first. We let $A_{t_j}B_{t_j}$ denote the registers that store the states for estimating $\text{Tr}(\rho^{t_j})$, where $t_j \in \Sigma_t$ and Σ_t includes all the indices of these registers.

Algorithm 2 Variational quantum Gibbs state preparation with truncation order K

- 1: Input: choose the ansatz of unitary $U(\boldsymbol{\theta})$, tolerance ε , truncation order K , and initial parameters of $\boldsymbol{\theta}$;
 - 2: Compute coefficients C_0, C_1, \dots, C_K according to Eq. (6).
 - 3: Prepare initial states $|00\rangle$ in registers AB and apply $U(\boldsymbol{\theta})$ to these states.
 - 4: Measure and compute $\text{Tr}(H\rho_{B_1})$ and compute the loss function $L_1 = \text{Tr}(H\rho_{B_1})$;
 - 5: Measure the overlap $\text{Tr}(\prod_{t_2 \in \Sigma_2} \rho_{B_{t_2}})$ via Destructive Swap Test and compute the loss function $L_2 = -\beta^{-1}C_1 \text{Tr}(\prod_{t_2 \in \Sigma_2} \rho_{B_{t_2}})$;
 - 6: Measure the overlap $\text{Tr}(\prod_{t_k \in \Sigma_k} \rho_{B_{t_k}})$ via higher order state overlap estimation and compute the loss function $L_k = -\beta^{-1}C_{k-1} \text{Tr}(\prod_{t_k \in \Sigma_k} \rho_{B_{t_k}})$ for each $k \in \{3, \dots, K+1\}$.
 - 7: Perform optimization of $\mathcal{F}_K(\boldsymbol{\theta}) = \sum_{k=1}^{K+1} L_k - \beta^{-1}C_0$ and update parameters of $\boldsymbol{\theta}$;
 - 8: Repeat 3-7 until the loss function $\mathcal{F}_K(\boldsymbol{\theta})$ converges with tolerance ε ;
 - 9: Output the state $\rho^{out} = \text{Tr}_A U(\boldsymbol{\theta})|00\rangle\langle 00|_{AB}U(\boldsymbol{\theta})^\dagger$;
-

II. TECHNICAL DETAILS

A. Analysis of the truncated free energy

Lemma S1 *Given the error tolerance $\epsilon > 0$ in the optimization problem in Eq. (8), suppose the truncation error of the free energy is $\delta_0 > 0$. Then we can derive a relation between $\mathcal{F}(\rho_G)$ and $\mathcal{F}_K(\rho(\boldsymbol{\theta}_0))$ below, where $\boldsymbol{\theta}_0$ is the output of the optimization and ρ_G is the Gibbs state.*

$$\mathcal{F}(\rho_G) \leq \mathcal{F}_K(\boldsymbol{\theta}_0) \leq \mathcal{F}(\rho_G) + \delta_0 + \epsilon. \quad (\text{S1})$$

Proof First, we show that left inequality in Eq. (S1). For arbitrary density operator ρ , we have $\mathcal{F}_K(\rho) - \mathcal{F}(\rho) > 0$. To be specific,

$$\mathcal{F}_K(\rho) - \mathcal{F}(\rho) = \beta^{-1}(S(\rho) - S_K(\rho)) \quad (\text{S2})$$

$$= -\beta^{-1} \text{Tr} \left(\sum_{j=K+1}^{\infty} \frac{(-1)^{j+1}}{j} (\rho - I)^j \rho \right) \quad (\text{S3})$$

$$= -\beta^{-1} \lim_{J \rightarrow \infty} \text{Tr} \left(\sum_{j=K+1}^J \frac{(-1)^{j+1}}{j} (\rho - I)^j \rho \right) \quad (\text{S4})$$

$$= \beta^{-1} \lim_{J \rightarrow \infty} \text{Tr} \left(\sum_{j=K+1}^J \frac{(-1)^j}{j} (\rho - I)^j \rho \right) \quad (\text{S5})$$

$$= \beta^{-1} \lim_{J \rightarrow \infty} \text{Tr} \left(\sum_{j=K+1}^J \frac{1}{j} (I - \rho)^j \rho \right) > 0. \quad (\text{S6})$$

In Eq. (S3), we expand the von Neumann entropy into the Taylor series, i.e., $S(\rho) = -\text{Tr}\left(\sum_{j=1}^{\infty} \frac{(-1)^{j+1}}{j} (\rho - I)^j \rho\right)$ and Eqs. (S4)-(S5) are due to the properties of limit.

Second, the right inequality in Eq. (S1) is a direct result of the definition of truncated free energy $\mathcal{F}_K(\rho)$.

$$\mathcal{F}_K(\boldsymbol{\theta}_0) - \mathcal{F}(\rho_G) = \mathcal{F}_K(\boldsymbol{\theta}_0) - \min_{\boldsymbol{\theta}} \mathcal{F}_K(\boldsymbol{\theta}) + \min_{\boldsymbol{\theta}} \mathcal{F}_K(\boldsymbol{\theta}) - \mathcal{F}(\rho_G) \quad (\text{S7})$$

$$\leq \epsilon + \mathcal{F}_K(\rho_G) - \mathcal{F}(\rho_G) \quad (\text{S8})$$

$$\leq \epsilon + \delta_0, \quad (\text{S9})$$

where we use that fact that $\min_{\boldsymbol{\theta}} \mathcal{F}_K(\boldsymbol{\theta}) \leq \mathcal{F}_K(\boldsymbol{\theta}_0) \leq \min_{\boldsymbol{\theta}} \mathcal{F}_K(\boldsymbol{\theta}) + \epsilon$ in Eq. (S8), and the inequality in Eq. (S9) is due to the truncation. \blacksquare

B. Estimation of the higher order gradients

Lemma S2 *Given a parameterized density operator $\rho(\boldsymbol{\theta})$, we have the following equality,*

$$\partial_{\theta_m} \text{Tr}(\rho(\boldsymbol{\theta})^3) = 3\partial_{\theta_{m,1}} \text{Tr}(\rho_1(\boldsymbol{\theta}) \otimes \rho_2(\boldsymbol{\theta}) \otimes \rho_3(\boldsymbol{\theta}) \cdot S_1 S_2), \quad (\text{S10})$$

where $\partial_{\theta_{m,1}}$ means the derivative is computed with respect to θ_m of the state stored in 1-th register, $\rho_j(\boldsymbol{\theta})$ is the state stored in j -th register, and $S_1 = \text{SWAP}_{12} \otimes I_3$ and $S_2 = I_1 \otimes \text{SWAP}_{23}$, and the SWAP_{ij} is the operator that swaps the state stored in i -th and j -th register.

Proof To prove the claim, we need the following result, which we give the proof later.

$$\text{Tr}(\rho_1 \otimes \rho_2 \otimes \rho_3 \cdot S_1 S_2) = \overline{\text{Tr}(\rho_2 \otimes \rho_1 \otimes \rho_3 \cdot S_1 S_2)} = \overline{\text{Tr}(\rho_3 \otimes \rho_2 \otimes \rho_1 \cdot S_1 S_2)}. \quad (\text{S11})$$

Let $\rho_1(\boldsymbol{\theta}) = \rho_2(\boldsymbol{\theta}) = \rho_3(\boldsymbol{\theta}) = \rho(\boldsymbol{\theta})$, then the claimed is proved in the following,

$$\frac{\partial}{\partial \theta_m} \text{Tr}(\rho(\boldsymbol{\theta})^3) = \frac{\partial}{\partial \theta_m} \text{Tr}(\rho_1(\boldsymbol{\theta}) \otimes \rho_2(\boldsymbol{\theta}) \otimes \rho_3(\boldsymbol{\theta}) \cdot S_1 S_2) \quad (\text{S12})$$

$$\begin{aligned} &= \frac{\partial}{\partial \theta_{m,1}} \text{Tr}(\rho_1(\boldsymbol{\theta}) \otimes \rho_2(\boldsymbol{\theta}) \otimes \rho_3(\boldsymbol{\theta}) \cdot S_1 S_2) \\ &+ \frac{\partial}{\partial \theta_{m,2}} \text{Tr}(\rho_1(\boldsymbol{\theta}) \otimes \rho_2(\boldsymbol{\theta}) \otimes \rho_3(\boldsymbol{\theta}) \cdot S_1 S_2) \\ &+ \frac{\partial}{\partial \theta_{m,3}} \text{Tr}(\rho_1(\boldsymbol{\theta}) \otimes \rho_2(\boldsymbol{\theta}) \otimes \rho_3(\boldsymbol{\theta}) \cdot S_1 S_2) \end{aligned} \quad (\text{S13})$$

$$\begin{aligned} &= \frac{\partial}{\partial \theta_{m,1}} \text{Tr}(\rho_1(\boldsymbol{\theta}) \otimes \rho_2(\boldsymbol{\theta}) \otimes \rho_3(\boldsymbol{\theta}) \cdot S_1 S_2) \\ &+ \frac{\partial}{\partial \theta_{m,2}} \text{Tr}(\rho_2(\boldsymbol{\theta}) \otimes \rho_1(\boldsymbol{\theta}) \otimes \rho_3(\boldsymbol{\theta}) \cdot S_1 S_2) \\ &+ \frac{\partial}{\partial \theta_{m,3}} \text{Tr}(\rho_3(\boldsymbol{\theta}) \otimes \rho_2(\boldsymbol{\theta}) \otimes \rho_1(\boldsymbol{\theta}) \cdot S_1 S_2) \end{aligned} \quad (\text{S14})$$

$$= 3 \frac{\partial}{\partial \theta_{m,1}} \text{Tr}(\rho_1(\boldsymbol{\theta}) \otimes \rho_2(\boldsymbol{\theta}) \otimes \rho_3(\boldsymbol{\theta}) \cdot S_1 S_2), \quad (\text{S15})$$

where the equality in Eq. (S13) is the result of chain rule, and we use the relation in Eq. (S11) to derive the equality in Eq. (S14).

Now we prove the equalities in Eq. (S11).

Let $\rho_1 = \sum_j p_j |\phi_j\rangle\langle\phi_j|$, $\rho_2 = \sum_l q_l |\psi_l\rangle\langle\psi_l|$, and $\rho_3 = \sum_k r_k |\xi_k\rangle\langle\xi_k|$. We have the following equalities.

$$\text{Tr}(\rho_1 \otimes \rho_2 \otimes \rho_3 \cdot S_1 S_2) = \sum_{jlk} p_j q_l r_k \langle\psi_l|\phi_j\rangle \langle\xi_k|\psi_l\rangle \langle\phi_j|\xi_k\rangle, \quad (\text{S16})$$

$$\text{Tr}(\rho_2 \otimes \rho_1 \otimes \rho_3 \cdot S_1 S_2) = \sum_{jlk} p_j q_l r_k \langle\phi_j|\psi_l\rangle \langle\xi_k|\phi_j\rangle \langle\psi_l|\xi_k\rangle, \quad (\text{S17})$$

$$\text{Tr}(\rho_3 \otimes \rho_2 \otimes \rho_1 \cdot S_1 S_2) = \sum_{jlk} p_j q_l r_k \langle\psi_l|\xi_k\rangle \langle\phi_j|\psi_l\rangle \langle\xi_k|\phi_j\rangle. \quad (\text{S18})$$

Comparing Eqs. (S16)-(S18), the equalities in Eq. (S11) are proved. \blacksquare

C. Proof for Proposition 5

Proposition 5 *Given the circuit in Fig. 3(b) and denote $\rho_B(\theta)$ its output state on system B. For the Ising chain model, if we compute its free energy in Eq. (3) and our truncated cost in Eq. (7), then the optimal θ 's that minimize these two loss functions are both*

$$\theta = \pi/2 + k\pi, \quad (\text{S19})$$

where $k \in \mathbb{Z}$. As a result, $\rho_B(\pi/2)$ is the best state, under this circuit, that approaching the Gibbs state in Eq. (51), and their fidelity could be larger than 95% for any $\beta \geq 1.25$.

Proof This claim can be directly derived by computing the global minimum of both loss functions \mathcal{F} and \mathcal{F}_2 using the ansatz in Fig. 3(b). Assuming $n_A = 1$, $n_B = n$ and denoting the output state as $|\psi\rangle_{AB}$, we can easily obtain the state ρ_B as

$$\rho_B(\theta) = \text{Tr}_A(|\psi\rangle\langle\psi|_{AB}) \quad (\text{S20})$$

$$= \cos^2(\theta/2)|0^n\rangle\langle 0^n|_B + \sin^2(\theta/2)|1^n\rangle\langle 1^n|_B. \quad (\text{S21})$$

To compute the derivatives of $\mathcal{F}(\theta)$ and $\mathcal{F}_2(\theta)$, we first present their explicit expressions.

$$\begin{aligned} \mathcal{F}(\theta) &= \text{Tr}(H_B \rho_B(\theta)) - \beta^{-1} S(\rho_B(\theta)) \\ &= \lambda_0 a + \lambda_1 b + \beta^{-1} [a \ln(a) + b \ln(b)], \end{aligned} \quad (\text{S22})$$

$$\begin{aligned} \mathcal{F}_2(\theta) &= \text{Tr}(H_B \rho_B(\theta)) + \beta^{-1} \left[2 \text{Tr}(\rho_B(\theta)^2) - \frac{1}{2} \text{Tr}(\rho_B(\theta)^3) - \frac{3}{2} \right] \\ &= \lambda_0 a + \lambda_1 b + \beta^{-1} \left[2a^2 + 2b^2 - \frac{a^3 + b^3}{2} - \frac{3}{2} \right], \end{aligned} \quad (\text{S23})$$

where we denote $\cos^2(\theta/2)$ by a and $\sin^2(\theta/2)$ by b , and λ_0 and λ_1 are the eigenvalues of H associated with eigenvectors $|0^n\rangle$ and $|1^n\rangle$, respectively.

Actually, in the Ising chain model, λ_0 and λ_1 are equal (c.f. Lemma S3). Thus, derivatives of $\mathcal{F}(\rho_B(\theta))$ and $\mathcal{F}_2(\rho_B(\theta))$ with respect to θ have the following form.

$$\partial_\theta \mathcal{F}(\theta) = \frac{\beta^{-1}}{2} \sin(\theta) (\ln(b) - \ln(a)) \quad (\text{S24})$$

$$\partial_\theta \mathcal{F}_2(\theta) = \frac{5\beta^{-1}}{2} \sin(\theta)(b - a). \quad (\text{S25})$$

From Eqs. (S24) (S25), the global minimums of \mathcal{F} and \mathcal{F}_2 are

$$\theta = \frac{\pi}{2} + k\pi \quad \forall k \in \mathbb{Z}. \quad (\text{S26})$$

The fidelity between $\rho_B(\pi/2)$ and ρ_G could be derived from Proposition 6 and Lemma S3, where if we set $N = 2^5$, $\Delta = 4$ and $\beta = 1.25$ and then we get $F(\rho_B(\pi/2), \rho_G) \geq 95.3\%$. Hence, we could achieve a fidelity higher than 95%, provided that $\beta \geq 1.25$. ■

D. Proof for Proposition 6

Proposition 6 *Given the circuit in Fig. 3(b) and let $\rho_B(\theta)$ be its output state on system B. Then the fidelity between $\rho_B(\pi/2)$ and the Gibbs state ρ_G is lower bounded. To be more specific,*

$$F(\rho_B(\pi/2), \rho_G) \geq \frac{1}{\sqrt{1 + (N/2 - 1)e^{-\beta\Delta}}}, \quad (\text{S27})$$

where N is the dimension of system B, i.e., $N = 2^{n_B}$ and Δ is the spectral gap of the Gibbs state ρ_G , i.e., the discrepancy between the minimum and the second minimum eigenvalues.

Proof To prove this result, we assume the eigenvalues, associated with the eigenvectors $|0\rangle, |1\rangle, \dots, |N-1\rangle$, for the Hamiltonian H are denoted by $\lambda_0, \lambda_1, \dots, \lambda_{N-1}$. Specifically, eigenvalues λ_0 and λ_{N-1} are associated with eigenvectors $|0^n\rangle$ and $|1^n\rangle$, respectively. A key feature of the Ising model is that $\lambda_0 = \lambda_{N-1}$ and they are minimum among all eigenvalues and let Δ denote the spectral gap of the Hamiltonian H_B , which implies $\lambda_j - \lambda_0 \geq \Delta$, where $j \neq 0, N-1$.

Let $\hat{\lambda}_j$ denote the eigenvalues of the Gibbs state. Then, according to the definition of Gibbs state, $\hat{\lambda}_j$ have the following form.

$$\hat{\lambda}_j = \frac{e^{-\beta\lambda_j}}{Z}. \quad (\text{S28})$$

where $Z = \sum_{l=0}^{N-1} e^{-\beta\lambda_l}$.

Next, we derive bounds on eigenvalues $\hat{\lambda}_0$ and $\hat{\lambda}_{N-1}$. Note that, in the Ising model, eigenvalues λ_0 and λ_{N-1} are equal, then the associated eigenvalues $\hat{\lambda}_0 = \hat{\lambda}_{N-1}$, and they have the explicit forms in the following.

$$\hat{\lambda}_0 = \hat{\lambda}_{N-1} = \frac{e^{-\beta\lambda_0}}{Z} \quad (\text{S29})$$

$$= \frac{1}{2 + \sum_{j \neq 0, N-1} e^{\beta(\lambda_0 - \lambda_j)}} \quad (\text{S30})$$

$$\geq \frac{1}{2 + (N-2)e^{-\beta\Delta}}. \quad (\text{S31})$$

Recall the output state of our algorithm is $\rho_B(\pi/2)$ in Proposition 5. The inequality in Eq. (S27) is immediately acquired by calculating the fidelity $F(\rho_B(\pi/2), \rho_G)$:

$$F(\rho_B(\pi/2), \rho_G) = \text{Tr} \sqrt{\rho_B^{1/2}(\pi/2) \rho_G \rho_B^{1/2}(\pi/2)} \quad (\text{S32})$$

$$= \text{Tr} \sqrt{1/\sqrt{2} \cdot \hat{\lambda}_0 \cdot 1/\sqrt{2} |0^n\rangle\langle 0^n| + 1/\sqrt{2} \cdot \hat{\lambda}_{N-1} \cdot 1/\sqrt{2} |1^n\rangle\langle 1^n|} \quad (\text{S33})$$

$$= \sqrt{2\hat{\lambda}_0} \quad (\text{S34})$$

$$\geq \frac{1}{\sqrt{1 + (N/2 - 1)e^{-\beta\Delta}}}. \quad (\text{S35})$$

This completes the proof. \blacksquare

The following lemma states some facts about the Ising model, which are helpful for the above proofs.

Lemma S3 *Given an Ising model Hamiltonian in Eq. (50), the eigenvalues λ_0 and λ_{N-1} , associated with eigenvectors $|0^{n_B}\rangle$ and $|1^{n_B}\rangle$, are equal, i.e., $\lambda_0 = \lambda_{N-1} = -L$. Particularly, the spectral gap is larger than 4 for all $n_B \geq 3$.*

Proof To prove that eigenvalues of $|0^{n_B}\rangle$ and $|1^{n_B}\rangle$ are equal, we compute their corresponding eigenvalues of each term $Z_{B,i}Z_{B,i+1}$. Notice that, for all $i = 1, \dots, L$,

$$Z_{B,i}Z_{B,i+1}|0^{n_B}\rangle = |0^{n_B}\rangle, \quad (\text{S36})$$

$$Z_{B,i}Z_{B,i+1}|1^{n_B}\rangle = |1^{n_B}\rangle. \quad (\text{S37})$$

Hence, in the Ising model, the eigenvalues of $|0^{n_B}\rangle$ and $|1^{n_B}\rangle$ are $-L$.

As for the rest eigenvectors $|j\rangle$, $j \neq 0, N-1$, their eigenvalues of $Z_{B,i}Z_{B,i+1}$ are given as follows.

$$Z_{B,i}Z_{B,i+1}|j\rangle = (-1)^{k_i+k_{i+1}}|j\rangle, \quad (\text{S38})$$

where k_i and k_{i+1} are the bits in the i -th and $(i+1)$ -th position of $|j\rangle$. Particularly, in the Ising model, the eigenvalue of $|j\rangle$ is represented as $-\sum_{i=1}^L (-1)^{k_{B,i}+k_{B,i+1}}$. To be specific,

$$H_B|j\rangle = -\sum_{i=1}^L (-1)^{k_i+k_{i+1}}|j\rangle. \quad (\text{S39})$$

Overall, the eigenvalues of $|j\rangle$ are larger than $-L$, which implies the eigenvalues of $|0^{n_B}\rangle$ and $|1^{n_B}\rangle$ are minimum.

Now we show that the spectral gap of the Ising model with more than 3 qubits is at least 4. The minimum eigenvalue of H_B is $-L$ means that $k_{B,i} + k_{B,i+1} = 0/2$ for all i , and hence the ground states are $|0^{n_B}\rangle$ and $|1^{n_B}\rangle$. If we flip one qubit of the eigenvector $|j\rangle$, then two terms like $(-1)^{k_{B,i}+k_{B,i+1}}$ of its eigenvalues will change by 2. If we flip more qubits, then more terms will change. Notice that the eigenvectors with eigenvalue larger than $-L$ will differ from those with minimum eigenvalue at least 1 qubit, resulting at least two terms change. Then, the overall difference between the minimum and second minimum eigenvalue is at least 4. \blacksquare